

Relative L X-Ray Fluorescence Cross-Sections in Heavy Elements In the Energy Region of 16-122 keV

Oğuz DOĞAN, Mehmet ERTUĞRUL, Önder ŞİMŞEK, Ümit TURGUT

*Atatürk University, K.K. Education Faculty Department of Physics,
25200, Erzurum-TURKEY*

Hasan ERDOĞAN

*Pamukkale University, Art and Science Faculty, Department of Physics,
Denizli-TURKEY*

Received 19.12.1997

Abstract

Relative L_1 , $L\alpha$, $L\beta$ and $L\gamma$ x-ray fluorescence cross-sections were observed in Ta, W, Re, Au, Hg, Tl, Pb, Bi, Th and U of 16.03, 17.78, 22.58, 25.77, 32.89, 38.18, 43.94, 50.21, 59.5 and 122 keV energies. In this study, L X-ray fluorescence cross-sections were measured at 59.5 and 122 keV and measured values of the other energies were taken from tables by Mann et. al. (1). The experimental relative fluorescence cross-sections were computed for the excitation energies 16.03, 17.78, 22.58, 25.77, 32.89, 38.18, 43.94, 50.21, 59.5 and 122 keV, compared with the theoretically calculated values by Scofield(11). The experimental results are found to agree with theory .

Introduction

The knowledge of L X-ray fluorescence cross-sections and their relative intensities for many elements are important in the fields of non-destructive testing, medical research, trace-element analysis and analysis of samples for geological where X-ray fluorescence (XRF) techniques are frequently used. The L shell X-ray fluorescence cross-sections of transitions to different L_1 , L_2 and L_3 subshells depend on the initial vacancy distribution controlled by the energy of excitation. Thus they depend on the different excitation energies. L x-ray production cross-sections can either be calculated from theoretical values of atomic parameters or determined experimentally. Calculations of L x-ray fluorescence cross-sections are made using theoretical or semi-empirical values of L subshell photoionization cross-sections, fluorescence yields, fractional emission rates and Coster-Kronig transition probabilities. Uncertainties in these tabulated quantities reflect the error in

L X-ray fluorescence cross-sections. For this reason, most users prefer the experimental values. For quantitative analytical applications it is necessary to know the different relative intensities of photons which contribute to the fluorescence. Since fluorescence cross-sections increase as the energy decreases, the contributions to X-ray fluorescence of low-energy, low-intensity transitions can be very important.

Some measurements of L1, $L\alpha$, $L\beta$ and $L\gamma$ x-ray production cross-sections in different elements by photons of various energies have been reported, [1-4]. In addition to these, the anisotropy of L-shell x-rays [5], M-shell x-ray production cross-sections and average fluorescence yield [6], the vacancy transfer probability dependence on L x-ray intensities [7] and $K\alpha$ to $L\alpha$ intensity ratio, and the enhancement factor of vacancy transfer [8] have been measured experimentally for several elements. These measurements have advantages of stable intensity and energy and of small sizes, which allow compact and efficient geometry, operates via a passive radiation source. The values of the cross-sections measured by various workers using different experimental arrangements are found to agree fairly well with one another as well as with the theoretically calculated values in the case of high-Z elements. However, some discrepancies among different measurements and calculated values are observed for intermediate-Z elements [1]. The theoretical calculations were made with fundamental physical parameters such as L-subshell ionisation cross-sections, fluorescence yields, Coster-Kronig transition probabilities, radiative decay rates and K to L shell vacancy transfer probabilities.

In this work, relative fluorescence cross-sections of L-subshell X-rays L1 (in 25.7 keV)/L1 (E), $L\alpha$ (25.7 keV) / $L\alpha$ (E), $L\beta$ (25.7 keV) / $L\beta$ (E) and $L\gamma$ (25.7 keV) / $L\gamma$ (E) were observed at excitation energies in 16.03, 17.78, 22.58, 25.77, 32.89, 38.18, 43.94, 50.21, 59.5 and 122 keV. The L1, $L\alpha$, $L\beta$ and $L\gamma$ x-ray production in 22 different elements with Z ranging 57-92 (La, Ce, Pr, Nd, Sm, Eu, Gd, Tb, Dy, Ho, Er, Yb, Lu, Ta, W, Au, Hg, Tl, Pb, Bi, Th and U) by the interval conversion K x-rays of Cu, Zn, Ge, Se, Rb, Zr, Mo, Ag, Sn, Ba, Nd, Gd and Er having weighted mean energies of 8.136, 16.03, 17.78, 22.58, 25.77, 32.89, 38.18, 43.94 and 50.214 keV were measured by Mann et al. [1]. They used secondary excitation method. The experimental results are in good agreement with theoretical values.

Experimental

The experimental arrangement for the annular source geometry in the direct excitation used in this study is shown in Fig.1. In this arrangement, low energy photon sources of ^{241}Am (100 mCi) and ^{57}Co (100 mCi) were used. The energy of primary photons are 59.5 and 122 keV, respectively. Spectroscopically pure targets of Ta (99%), W (99%), Re (99%), Au (99.99%), $\text{Hg}(\text{NO}_3)_2$ (99.9%), Tl_2O_3 (99%), PbO (99.95%), Bi_2O_3 (99.98%), $\text{Th}(\text{NO}_3)_2$ (99%) and $(\text{CH}_3\text{COO})_2\text{UO}_2 \cdot 2\text{H}_2\text{O}$ (99%) of thickness ranging from 25.84 to 51.68 mg/cm^2 , 3.5 μm thick Mylar backing have been used for measurements. We have also cross-checked the thickness by measuring the K X-ray yields from the targets excited by 59.5 and 122 keV photons emitted from an annular sources of ^{241}Am and ^{57}Co . The L X-ray spectra from various targets were recorded with a Si(Li) detector

(FWHM=160 eV at 5.96 keV, active area=12.5 mm², sensitive depth = 3.5 mm, Be window thickness=12.5 μm) coupled to a Nuclear Data MCA system (ND66B) based 4096 channels analyser through a spectroscopy amplifier. Each target was excited and data was subsequently recorded over time intervals ranging from 3 to 12 h. A typical X-ray spectra for Bi is shown in Fig. 2. The peaks due to the L1, Lα, Lβ and Lγ group of lines are well resolved.

Data Analysis

The experimental L X-ray fluorescence cross-sections σ_L^x were evaluated using the relation

$$\sigma_L^x = \frac{N_L}{I_0 G \varepsilon_L \cdot \beta_L \cdot m}, \quad (1)$$

where N_L is the number of counts per unit time under the photopeak corresponding to L x-ray of the element; the product $I_0 G$ is the intensity of the exciting radiation falling on the area of the target sample visible to the detector; ε_L is the efficiency of the Si(Li) detector at the average L X-ray energy of the element; and m is the mass per unit area of the element in g/cm². The β_L is the self-absorption correction factor for the incident photons and emitted L X-ray photons. The values of β_L have been calculated by using the following expression obtained by assuming that the fluorescent X-rays are incident normally at the detector [9]:

$$\beta_L = \frac{1 - \exp[(-1) \cdot (\mu_{inc} \sec \theta_1 + \mu_{emt} \sec \theta_2) m]}{(\mu_{inc} \sec \theta_1 + \mu_{emt} \sec \theta_2) m} \quad (2)$$

where μ_{inc} and μ_{emt} are the absorption coefficients at the incident and emitted x-ray photon energy, for which values are taken from the tables of Storm and Israel [10]; m is the thickness of the target in g/cm²; $\theta_1 (=45^\circ)$ and $\theta_2 (=0^\circ)$ are the angles of incident photons and emitted X-rays with respect to the normal at the surface of the sample.

However, in the present work, the value of the factor $I_0 G \varepsilon_{Li}$, which contains terms related to the incident photon flux, geometrical factor and the absolute efficiency of the X-ray detector, was determined by collection the K X-ray spectra of thin samples of Fe (99.9%), ZnO₂ (99.9%), As₂O₃ (99.9%), SeO₂ (99%), SrCl₂ · 6H₂O (99%), ZrO₂ (99.9), Mo (99.9%) and Pd₂Cl (99%) in the same geometry in which the L XRF cross-sections were measured using the equation

$$I_0 G \varepsilon_{K\alpha} = \frac{N_{K\alpha}}{\sigma_{K\alpha} \cdot \beta_{K\alpha} \cdot m}, \quad (3)$$

where $I_{K\alpha}$, $\beta_{K\alpha}$ and $\varepsilon_{K\alpha}$ have the same meaning as in Eqn. (1), except that they correspond to K X-rays instead of the i th group of L X-rays. In these calculations, the theoretical values of K X-ray fluorescence cross-sections ($\sigma_{k\alpha}$) were calculated using the equation

$$\sigma_{K\alpha} = \sigma_K(E) \cdot \omega_K \cdot F_{K\alpha}, \quad (4)$$

where $\sigma_K(E)$ is the K shell photoionisation cross-sections (11) for the elements at the excitation energy E, ω_K is the K shell fluorescence yield from the tables of Krause [12] and $F_{K\alpha}$ is the fractional X-ray emission rate for $K\alpha$ X-rays and is defined as

$$F_{K\alpha} = \left(1 + \frac{IK\beta}{IK\alpha}\right)^{-1}, \quad (5)$$

where $IK\beta/IK\alpha$ is the $K\beta$ to $K\alpha$ X-ray intensity ratio [13]. It is worth mentioning that the measured values are found to agree well with theoretical values. It is therefore valid to take experimental or theoretical values of K X-ray fluorescence cross-sections for the evaluation of I_0G_ε values. The measured and fitted values of I_0G_ε have also been plotted as a function of K X-ray energy [6.4 keV (Fe $K\alpha$), 7.05 keV(Fe $K\alpha$), 8.63 keV(Fe $K\alpha$), 9.57 keV(Fe $K\alpha$), 11.21 keV(Fe $K\alpha$), 12.5 keV(Fe $K\alpha$), 14.14 keV(Fe $K\alpha$), 15.74 keV(Fe $K\alpha$), 17.44 keV(Fe $K\alpha$), 17.7 keV(Fe $K\alpha$), 19.64 keV(Fe $K\alpha$), 21.12 keV(Fe $K\alpha$) and 23.87 keV(Fe $K\alpha$)] in Fig. 3.

Theoretical L X-Ray Cross-Section

In this work we have calculated the theoretical relative L X-ray fluorescence cross-sections for the elements in the atomic number range $73 \leq Z \leq 92$ at all the incident photon energies using the following equations:

$$\frac{\sigma_{L1,\alpha}(25.7)}{\sigma_{L1,\alpha}(E)} = \frac{[\sigma_3^* + \sigma^*K\eta_{KL3} + (\sigma_2^* + \sigma^*K\eta_{KL2})f_{23} + (\sigma_1^* + \sigma^*K\eta_{KL1})(f_{13} + f_{12}f_{23})]}{[\sigma_3 + \sigma_K\eta_{KL3} + (\sigma_2\sigma_K\eta_{KL2})f_{23} + (\sigma_1 + \sigma_K\eta_{KL1})(f_{13} + f_{12}f_{23})]} \\ (\sigma_1^* + \sigma^*K\eta_{KL1})\omega_1F_{1\beta} + [(\sigma_2^* + \sigma^*K\eta_{KL2}) + (\sigma_1^* + \sigma^*K\eta_{KL1})(f_{12})]\omega_2F_{2\beta} +$$

$$\frac{\sigma_{L\beta}(25.7)}{\sigma_{L\beta}(E)} = \frac{[\sigma_3^* + \sigma^*K\eta_{KL3} + (\sigma_2^* + \sigma^*K\eta_{KL2})f_{23} + (\sigma_1^* + \sigma^*K\eta_{KL1})(f_{13} + f_{12}f_{23})]}{[\sigma_3 + \sigma_K\eta_{KL3} + (\sigma_2\sigma_K\eta_{KL2})f_{23} + (\sigma_1 + \sigma_K\eta_{KL1})(f_{13} + f_{12}f_{23})]} \\ (\sigma_1 + \sigma_K\eta_{KL1})\omega_1F_{1\beta} + [(\sigma_2 + \sigma_K\eta_{KL2})f_{23} + (\sigma_1 + \sigma_K\eta_{KL1})(f_{13} + f_{12}f_{23})]$$

$$\frac{\sigma_{L\gamma}(25.7)}{\sigma_{L\gamma}(E)} = \frac{(\sigma_1^* + \sigma^*K\eta_{KL3})\omega_1F_{1\gamma} + [(\sigma_2^* + \sigma^*K\eta_{KL2}) + (\sigma_1^* + \sigma^*K\eta_{KL1})f_{12}]\omega_2F_{2\gamma}}{(\sigma_1 + \sigma_K\eta_{KL1})\omega_1F_{1\gamma} + [(\sigma_2 + \sigma_K\eta_{KL2}) + (\sigma_1 + \sigma_K\eta_{KL1})f_{12}]\omega_2F_{2\gamma}}$$

* represents cross-section relative to energy of 25.7 keV

where σ_1 , σ_2 and σ_3 are the photoionisation cross-sections of the subshells L_1 , L_2 and L_3 , respectively; ω_1 , ω_2 and ω_3 are the corresponding subshell fluorescence yields; η_{k11} , η_{k12} , η_{k13} are K shell to L_1 , L_2 , and L_3 subshell vacancy transfer probabilities; F_{ij} (F_{31} , $F_{3\alpha}$, $F_{3\beta}$, ... *etc.*) are the fractions of the radiation transitions of the subshell L_i (L_1 , L_2 and L_3) contained in the j th spectral line i.e.,

$$F_i = \frac{[\Gamma_3(X - L_i)]}{\Gamma_i},$$

Table 1. Relative L x-ray intensity
E- means experimentally T-means theoretically

Ele	I. Ratio	16.03 keV	17.7 keV	22.5 keV	25.7 keV	32.8 keV	38.1 keV	43.9 keV	50.2 keV	59.5 keV	122.6 keV
	E	0.26	0.35	0.75	1	1.89	2.90	-	-	12.1	-
	L1/L1 T	0.26	0.35	0.68	1	2.02	3.12	-	-	12.2	11.2
Ta	E	0.25	0.36	0.72	1	2.02	3.18	-	-	11.9	11.3
	L α /L α T	0.26	0.35	0.68	1	2.01	3.09	-	-	12.3	11.1
	E	0.28	0.38	0.73	1	1.89	2.85	-	-	9.54	13.8
	L β /L β T	0.29	0.38	0.71	1	1.87	2.78	-	-	9.41	14.2
	E	0.29	0.39	0.71	1	1.75	2.54	-	-	8.04	16.7
	L γ /L γ T	0.31	0.40	0.72	1	1.82	2.66	-	-	7.97	15.7
W	E	0.26	0.39	0.70	1	1.95	3.00	-	-	12.2	-
	L1/L1 T	0.28	0.37	0.73	1	2.09	3.33	-	-	13.0	11.2
	E	0.29	0.39	0.79	1	2.09	3.44	-	-	13.0	12.8
	L α /L α T	0.29	0.39	0.76	1	2.24	3.46	-	-	13.9	12.1
	E	0.33	0.44	0.80	1	1.94	3.06	-	-	10.7	14.4
	L β L β T	0.33	0.42	0.78	1	2.07	3.06	-	-	10.3	15.5
	E	0.36	0.48	0.88	1	2.02	3.22	-	-	10.1	21.1
	L γ L γ T	0.34	0.43	0.78	1	2.59	2.86	-	-	9.93	18.5
	E	0.31	0.41	0.77	1	2.10	3.19	4.88	-	10.7	-
	L1/L1 T	0.28	0.37	0.73	1	1.95	2.94	4.36	-	11.6	13.4
	E	0.30	0.39	0.73	1	2.00	2.98	4.34	-	10.9	14.3
	L α /L α T	0.28	0.36	0.71	1	1.94	2.94	4.34	-	11.0	12.9
Au	E	0.30	0.38	0.73	1	1.92	2.80	4.04	-	10.5	13.2
	L β L β T	0.30	0.37	0.71	1	1.89	2.80	4.08	-	9.66	13.8
	E	0.33	0.42	0.73	1	1.99	2.84	3.79	-	10.4	18.6
	L γ L γ T	0.31	0.40	0.69	1	1.85	2.72	3.91	-	9.37	15.7
	E	0.27	0.35	0.68	1	1.72	2.52	3.71	-	9.67	-
	L1/L1 T	0.28	0.37	0.71	1	1.93	2.93	4.33	-	9.66	11.5

Hg	E	0.29	0.40	0.72	1	1.87	3.03	4.35	-	10.5	13.4
	L α L α										
T	E	0.28	0.37	0.70	1	1.92	2.92	4.31	-	10.3	12.4
	L β L β										
T	E	0.29	0.40	0.72	1	1.87	2.92	4.17	-	9.98	12.9
	L β L β	0.30	0.38	0.71	1	1.86	2.80	4.07	-	9.72	13.6
T	E	0.33	0.44	0.79	1	1.94	3.08	3.88	-	9.59	15.4
	L γ L γ	0.31	0.40	0.72	1	1.84	2.73	3.93	-	9.56	15.5
T	E	0.27	0.36	0.72	1	1.72	2.87	4.18	5.11	9.68	-
	L1/L1	0.28	0.37	0.69	1	1.92	2.85	4.27	6.18	10.3	12.3
T1	E	0.28	0.37	0.72	1	1.81	2.76	4.02	5.92	9.91	13.6
	L α L α	0.28	0.37	0.70	1	1.91	2.90	4.29	6.20	9.79	12.0
T	E	0.29	0.37	0.71	1	1.78	2.77	4.01	5.63	9.35	12.1
	L β L β	0.30	0.39	0.71	1	1.86	2.79	4.06	5.80	9.28	12.5
T	E	0.28	0.39	0.69	1	1.77	2.61	3.46	5.05	8.53	14.4
	L γ L γ	0.31	0.40	0.71	1	1.83	2.70	3.92	5.55	8.63	13.4
T	E	0.29	0.38	0.74	1	1.76	2.94	4.47	5.59	10.0	-
	L1/L1	0.28	0.37	0.70	1	1.91	2.89	4.26	6.15	10.3	12.2
T	E	0.29	0.39	0.76	1	1.96	3.05	4.34	5.78	10.5	14.8
	L α L α	0.28	0.37	0.70	1	1.91	2.90	4.27	6.16	10.2	12.5
T	E	0.30	0.38	0.74	1	1.90	2.88	4.10	5.53	9.78	12.9
	L β L β	0.30	0.39	0.71	1	1.86	2.78	4.04	5.77	9.55	13.2
T	E	-	0.38	0.73	1	0.81	2.87	3.36	4.87	9.26	14.5
	L γ L γ	0.31	0.40	0.71	1	1.83	2.71	3.91	5.51	8.88	14.2
Bi	E	-	0.36	0.67	1	1.75	2.97	3.69	5.09	9.81	-
	L1/L1	-	0.37	0.70	1	1.93	2.92	4.30	6.16	9.76	6.86
T	E	-	0.36	0.73	1	1.80	2.91	4.21	5.78	10.1	13.8
	L α L α	-	0.37	0.70	1	1.91	2.90	4.26	6.14	9.68	6.70
T	E	-	0.38	0.73	1	1.79	2.85	4.07	5.38	9.45	12.6
	L β L β	-	0.39	0.71	1	1.85	2.77	4.03	5.75	8.84	7.21
T	E	-	0.41	0.74	1	1.81	2.96	3.92	5.46	8.82	14.3
	L γ L γ	-	0.40	0.72	1	1.82	2.69	3.89	5.50	9.12	7.93

Th	E	-	-	0.73	1	1.98	2.94	4.33	5.86	10.7	14.4
	L ₁ /L ₁	-	-	0.70	1	1.88	2.85	4.18	6.03	10.2	6.87
	T	-	-	0.70	1	1.88	2.85	4.18	6.03	10.2	6.87
	E	-	-	0.73	1	1.94	3.26	4.15	6.08	10.2	17.6
	L _α L _α	-	-	0.70	1	1.89	2.85	4.18	6.01	9.93	6.84
	T	-	-	0.70	1	1.89	2.85	4.18	6.01	9.93	6.84
U	E	-	-	0.77	1	1.94	2.89	4.05	5.72	9.57	17.8
	L _β L _β	-	-	0.72	1	1.82	2.69	3.88	5.49	9.42	7.91
	T	-	-	0.72	1	1.82	2.69	3.88	5.49	9.42	7.91
	E	-	-	0.77	1	1.96	2.82	3.69	5.66	8.90	20.3
	L _γ L _γ	-	-	0.73	1	1.78	2.61	3.72	5.23	8.77	8.90
	T	-	-	0.73	1	1.78	2.61	3.72	5.23	8.77	8.90
	E	-	-	0.69	1	1.98	3.00	3.83	5.97	10.3	14.6
	L ₁ /L ₁	-	-	0.70	1	1.90	2.85	4.13	5.96	10.0	13.6
	T	-	-	0.70	1	1.90	2.85	4.13	5.96	10.0	13.6
	E	-	-	0.69	1	1.89	2.83	4.10	5.94	9.94	16.2
L _α L _α	-	-	0.70	1	1.90	2.84	4.16	5.96	9.60	13.1	
T	-	-	0.70	1	1.90	2.84	4.16	5.96	9.60	13.1	
E	-	-	0.69	1	1.80	2.75	3.77	5.35	8.84	16.1	
L _β L _β	-	-	0.72	1	1.83	2.69	3.84	5.42	8.65	14.2	
T	-	-	0.72	1	1.83	2.69	3.84	5.42	8.65	14.2	
E	-	-	-	1	1.75	2.70	3.93	4.81	8.25	15.4	
L _γ L _γ	-	-	-	1	1.75	2.70	3.93	4.81	8.25	15.4	
T	-	-	0.73	1	1.79	2.58	3.67	5.12	8.22	15.2	

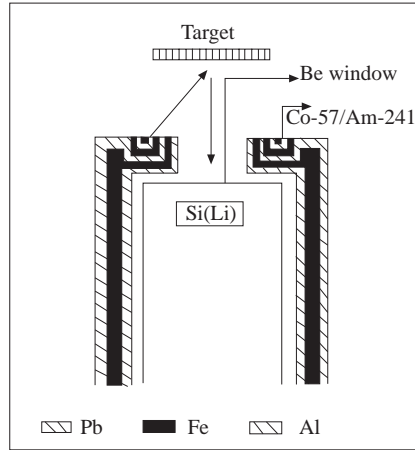


Figure 1. Experimental set-up

where Γ_i is the total radiative width of Li. The parameters f_{12} , f_{13} and f_{23} are the Coster-Kronig transition probabilities for $L_1 \rightarrow L_2$, $L_2 \rightarrow L_3$, $L_1 \rightarrow L_3$, respectively.

For these calculations, photoionisation cross-sections (σ_{Li}) were taken from the tables of Scofield [11]. ω_i and f_{ij} were taken from the tables of Krause [12].

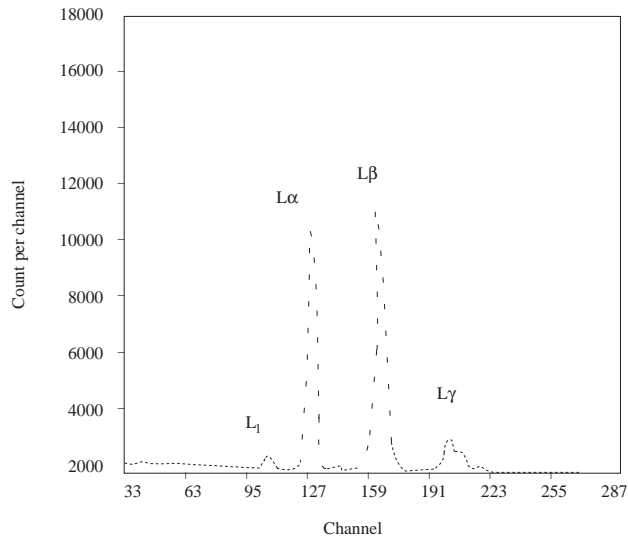


Figure 2. L x-ray spectra of Bi

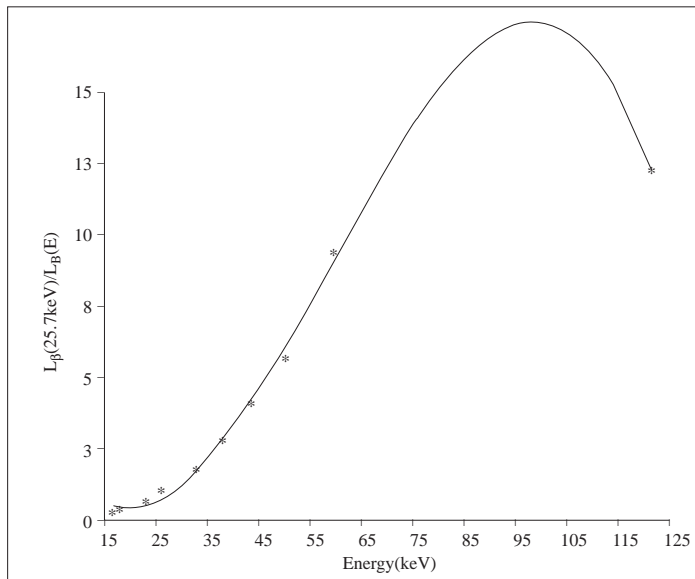


Figure 3. $I_0 G \varepsilon$ versus mean K x-ray energy (keV)

Result and Discussion

The values of the relative L x-ray fluorescence cross sections ($\sigma_{Li}(25.7) / \sigma_{Li}(E)$, $\sigma_{L\alpha}(25.7) / \sigma_{L\alpha}(E)$, $\sigma_{L\beta}(25.7) / \sigma_{L\beta}(E)$ and $\sigma_{L\gamma}(25.7) / \sigma_{L\gamma}(E)$) for Ta, W, Re, Au, Hg, Pb, Tl, Bi, Th and U at different excitation energies are listed in Table 1. The L x-ray fluorescence cross-sections were measured at 59.5 and 122 keV excitation energies and measured values of the other excitation energies were taken from tables by Mann's et al. [1] table. The experimental values of the relative L x-ray fluorescence cross-sections were compared with the theoretical values which were calculated by Scofield [11] at the same energies. The experimental results agree with theoretical results. Figure 1 shows $\sigma_{L\beta}(25.7) / \sigma_{L\beta}(E)$ fluorescence cross section as a function of atomic number and Fig. 2 shows $\sigma_{L\beta}(25.7) / \sigma_{L\beta}(E)$ fluorescence cross section as a function of the energy. It is interesting that there is agreement although the $\sigma_{L\beta}(25.7) / \sigma_{L\beta}(E)$ fluorescence cross-section is rising with the energy.

The overall error in the measured L x-ray fluorescence cross section is estimated to be of the order of 5-10%. The error is attributed to the uncertainties in different parameters used to evaluate L x-ray fluorescence cross-sections as follow. The error in the area evaluation under the L x-ray peak is less than 2%; in the detector efficiency, 3% or less; in the thickness measurement, about 2% in the I_0G factor, of the order of 5%; and in the absorption correction factor (β), on the order of 2%.

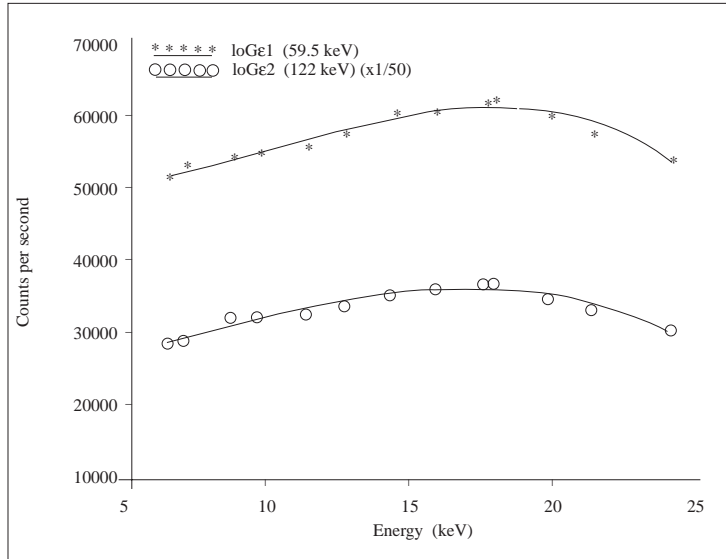


Figure 4. Relative intensity of L β x-ray versus excitation energy (keV)

References

- [1] K. S. Mann, N. Singh, R. Mittal, B. S. Sood, K. L. Allawadhi and K. L. Allawadhi, X-Ray Spectrometry, 23 (1994) 208.
- [2] D. V. Rao, R. Cesareo and G. E. Gigante, X-Ray Spectrometry, 22 (1993) 401.
- [3] K. S. Mann, N. Singh, R. Mittal, B. S. Sood and K. L. Allawadhi, J. Phys, B 1923 (1990) 3521.
- [4] M. L. Garg, D. Mehta, H. R. Verma, N. Singh, P. C. Mangal and P. N. Trehan, J. Phys, B19 (1986) 1615.
- [5] M. Ertuğrul, E. Büyükkasap, A. Küçükönder, A. I., Kopya and H. Erdoğan, Nuovo Cimento, 17D (1995) 993.
- [6] M. Ertuğrul, E. Tıraşoğlul, Y. Kurucu, S. Erzenoğlu, R. Durak and Y. Şahin, Nucl. Instrum. Meth. B, 108 (1996) 18.
- [7] M. Ertuğrul, Nucl. Instrum. Meth. B (in press),
- [8] M. Ertuğrul, J. Phys. B: At. Mol. Opt. Phys., 28 (1995) 4037.
- [9] M. Ertuğrul, E. Büyükkasap, H. Erdoğan and Y. Şahin, Doğa Tr. J. of Physics, 522, 19 (1991).
- [10] E. Storm and I. Israel, Nucl. Data Tables A7, 565 (1970).
- [11] J. H. Scofield, UCRL, No: 51362 (1973).
- [12] M. O. Krause, J. of Phys. and Chem. Ref. Data 8, 3307 (1979).
- [13] J. H. Scofield, At. Data and Nucl. Data Tables 14, 121 (1974).